Effect of Nuclear Motion on Molecular High-Order Harmonics and on Generation of Attosecond Pulses in Intense Laser Pulses

André D. Bandrauk, Szczepan Chelkowski, Shinnosuke Kawai, and Huizhong Lu
Département de Chimie, Université de Sherbrooke, Sherbrooke, Qc, J1K 2R1 Canada
(Received 21 March 2008; published 6 October 2008)

We calculate harmonic spectra and shapes of attosecond-pulse trains using numerical solutions of Non-Born-Oppenheimer time-dependent Shrödinger equation for 1D H_2 molecules in an intense laser pulse. A very strong signature of nuclear motion is seen in the time profiles of high-order harmonics. In general the nuclear motion shortens the part of the attosecond-pulse train originating from the first electron contribution, but it may enhance the second electron contribution for longer pulses. The shape of time profiles of harmonics can thus be used for monitoring the nuclear motion.

DOI: 10.1103/PhysRevLett.101.153901 PACS numbers: 42.65.Ky, 32.80.Rm, 42.50.Hz, 42.65.Re

High-order harmonic generation, is one of the most studied effects of the nonlinear nonperturbative response of atoms and molecules [1,2] to short intense laser pulses with the results that the coherent emitted light can be harnessed to produce new coherent trains of extremely short, ''attosecond'', pulses, on the time scale of electron motion [1,3]. A simple model, based on the idea of tunnelling ionization of an electron in an atom followed by the laser control of recollision of the ionized electron with the parent ion allow for interpreting the harmonic generation process in terms of recolliding electron trajectories [4] and leads to a universal cutoff law for the maximum in photon energy in harmonic generation. Molecules introduce a further complexity in harmonic generation due to nuclear motion and charge resonance enhanced ionization, CREI [5,6], at distances larger than equilibrium. Further complexity arises due to distortion of the molecular structures by a phenomenon called bond softening [7], as well as, by the influence of the charge transfer states like H^+H^- in enhanced ionization [2] of the H_2 molecule. Recently molecular high-order harmonic generation, MHOHG [2], has been proposed as a novel method for orbital tomography [8] and comparison of isotope effects on relative intensities of MHOHG in H_2 and D_2 has suggested the possibility of observing nuclear wave packet motion on a subcycle, near-fs time scale [9,10], since the time for recollision and recombination of the ionized electron is well predicted by the recollision model as $2/3$ of the laser cycle in the cutoff region of the harmonic spectrum [4].

In the present work we reexamine MHOHG using a time-frequency profile analysis [11] which allows us to identify recollision times [2] in concert with the evolution of nuclear wave packets during the harmonic generation process. In addition, the time-profile analysis of harmonics gives us direct information about relative intensities of individual attosecond pulses present inside the pulse train generated via experimental frequency filtering of harmonics [3]. Our analysis suggests that molecular motion may play the role of an important *time-gating* allowing to shorten the trains of generated attosecond pulses. We also show that time profiles of harmonics can be used for monitoring the nuclear wave packet motion. Both these effects rely on the very rapid increase of ionization rate and of harmonic efficiency as function of internuclear distance R. This time-gating effect is mostly due to the complete depopulation of the initial state from which the electron tunnels at later stage of molecular dissociation, leading to the termination of the harmonic generation process at earlier time than in atoms with a similar ionization potentials I_p as the molecules at the equilibrium internuclear distance. Most past theoretical studies of MHOHG were restricted to the frozen nuclei case (Born-Oppenheimer), and to our knowledge no dynamic (TDSE) studies of of harmonic time profiles in a moving H_2 (or even in H_2^+) molecule were ever performed. Our present study of MHOHG is based on a full 1D, two-electron non-Born-Oppenheimer simulations of H_2 in a short intense laser pulse. Similar calculations for H_2 and HD were performed earlier by Kreibich *et al.* [12] who calculated harmonic spectra alone. We extend here our previous static studies of two-electron dynamics [13] by including fully the 1D nuclear motion in TDSE via two electron coordinates (z_1, z_2) and one nuclear coordinate R. The complete 1D TDSE is written as (in a.u. $e = \hbar = m_e = 1$)

$$
\begin{aligned}
i\frac{\partial \psi(t)}{\partial t} &= [H_e + H_N + E(t)(z_1 + z_2)]\psi(t), \\
H_e &= \sum_{i=1}^{2}\left[-\frac{1}{2}\frac{\partial^2}{\partial z_i^2} - V_+(z_i) - V_-(z_i) + V_{\mathrm{rep}}\right], \\
V_\pm(z_i) &= [(z_i \pm R/2)^2 + c]^{-(1/2)}, \\
V_{\mathrm{rep}} &= (z_1 - z_2)^2 + d]^{-(1/2)}, \quad H_N = -\frac{1}{2\mu}\frac{\partial^2}{\partial R^2} + \frac{1}{R}, \\
E(t) &= \varepsilon(t)\sin(\omega_L t),
\end{aligned}
\tag{1}
$$

where μ is the reduced mass of two nuclei. The Coulomb softening parameters c, d are chosen to reproduce faithfully the first three electronic potentials of H_2 ($c = 0.7$, $d = 1.2375$), [13]. The TDSE, Eq. (1), is solved using a

split operator spectral method [14] for the laser pulses of frequency ω_L and the pulse envelope $\varepsilon(t)$. We used the electron grid of size $|z_k| < 512$ a.u. containing 4096 grid points for each electron and the nuclear grid of size $R <$ 12 a.u. containing 160 grid points. For very short pulses we used the electron wave function is still well contained within the grid. We verified that the absorber which was introduced in the electron grid led to a few percent loss of the norm near the end of the pulse. The complete numerical two-electron nuclear wave function is then used to obtain the laser induced electron dipole moment $d(t) = \langle\psi(t)|(z_1 + z_2)|\psi(t)\rangle$. The Fourier transform of the total dipole $d(t)$ gives the MHOHG power spectrum $|d_F(\omega)|^2$. The time profile of harmonics, obtained via a Gabor transform $d_G(\omega, \beta)$ is calculated using Eqs. (3) and (4) from Ref. [11], where β is the central time of the Gaussian time-window $G(t - \beta) = \exp(-(t - \beta)^2/2\sigma_0^2)$, with $\sigma_0 =$ 0.1 fs. In the frequency domain, this time-window corresponds to a Gaussian frequency filter with a spectral width $= 10\omega_L$ at its half-maximum for the laser wavelength 800 nm used here. The time-profile analysis [11] provides the recollision time τ_c [1,3,11] of the electron during the dissociative ionization process, and informs us about the depopulation of the state to which the electron returns. At fixed $\omega = \omega_c$ the function $d_G(\omega_c, t)$ describes the shape of the attosecond-pulse train generated via synthetizing about eight harmonics centered around ω_c. Finally, integrating out the probability distribution $|\psi(t)|^2$ over both electron coordinates $z_{1,2}$ gives the time-dependent nuclear wave packet distributions $P_N(R, t)$ during the process.

We show in Fig. 1 the MHOHG generated by a 6-cycle laser pulse, shown in Fig. 3(e), at intensity $I = 10^{15}$ W/cm^2 and wavelength 800 nm. Figure 1(a) shows MHOGH in the plateau region and Fig. 1(b) shows the near cutoff region. We have also solved the 2-electron TDSE (1) for the static case at the equilibrium value $R = R_e$ which in our 1D molecule is equal to 1.7 a.u. [13]. The harmonic intensities in this static case, shown in Fig. 1(c) (solid-lines), are at least 1 order of magnitude stronger than harmonics in the moving H_2 case (dashed). Much more significant effects due to the nuclear motion occur in the harmonic time profiles shown in Fig. 2. Note that the overall shape of harmonic spectra (Fig. 1) is not significantly modified by the nuclear motion which in general lowers the harmonic intensities by a nearly constant factor. By contrast, the shape of the time profiles is significantly affected by the nuclear motion. We show in Figs. 2(b)–2(d) the MHOHG time profiles as functions of time for three selected harmonic orders: 65th (plateau), 121th and 139th (cutoff region) as indicted in the left corner. The highest one is indeed very close to the cutoff. For each case we plot the time-profiles for D_2, H_2 and for the frozen nuclei case (static). We also plot in Fig. 2(a). the "survival" probability of a neutral molecule defined as the probability of finding both electrons at $|z_k| < 6$ a.u. When this probability falls below 0.1 and when we still see a significant harmonic signal it most likely originates from the H_2^+ MHOHG. We note that the lower order harmonic, (the 65th) shows that the nuclear motion simply terminates the harmonic generation at $t = 3.5$ cycles, the subsequent peaks seen in our logarithmic scale are relatively weak for this harmonic. By contrast, the time profiles of higher orders (121th and 139th, close to the cutoff region) for moving nuclei exhibit a deep minimum at $t = 3.5$ cycles whereas the profiles for the static case show a much slower decrease with no minimum. This minimum occurs when the survival probability of the neutral molecule falls to below 0.1. We checked that at this time the "existence" probability of H_2^+ is still huge since it is equal to 0.8 (the latter is defined as a probability of finding $|z_1| < 6$ a.u. and $|z_2| > 6$ a.u. plus vice versa). Therefore, it seems reasonable to interpret the subsequent rise (at $t > 3.5$ cycles) of the time-profile as a contribution of the second electron (from H_2^+) to the harmonic signal. We checked that similar deep minimum occurs for time profiles for all orders higher than 100 whereas for lower orders the trains are simply shortened. Thus time-profile analysis allows us to distinguish the contribution from the second electron. This would be more difficult to see in atoms than in molecules

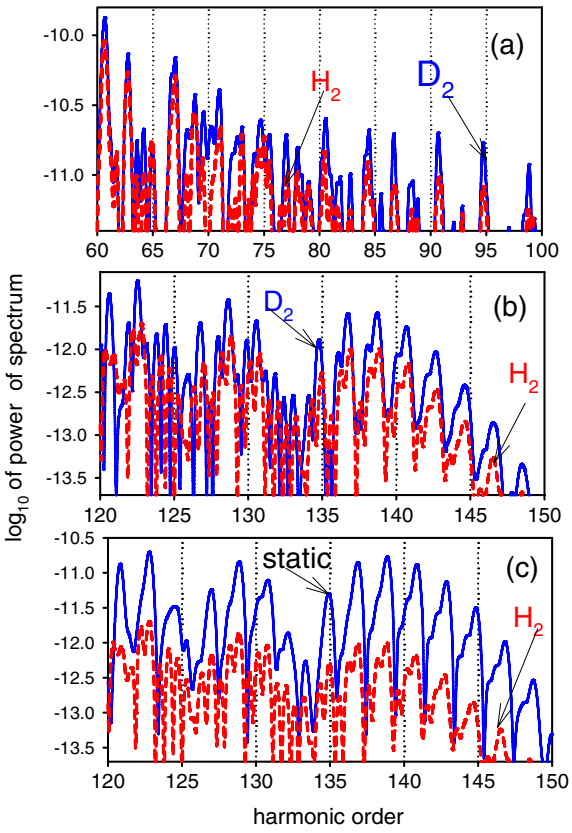

FIG. 1 (color online). Harmonic spectra obtained from Eq. (1) for moving H_2 and D_2 molecules. (a) plateau region and in (b), (c) cutoff region. (c) the static case (solid lines), obtained for R fixed at $R_e = 1.7$ a.u. In Figs. 1–3: $I = 10^{15}$ W/cm^2, $\lambda =$ 800 nm and the laser electric field is shown in Fig. 3(d).

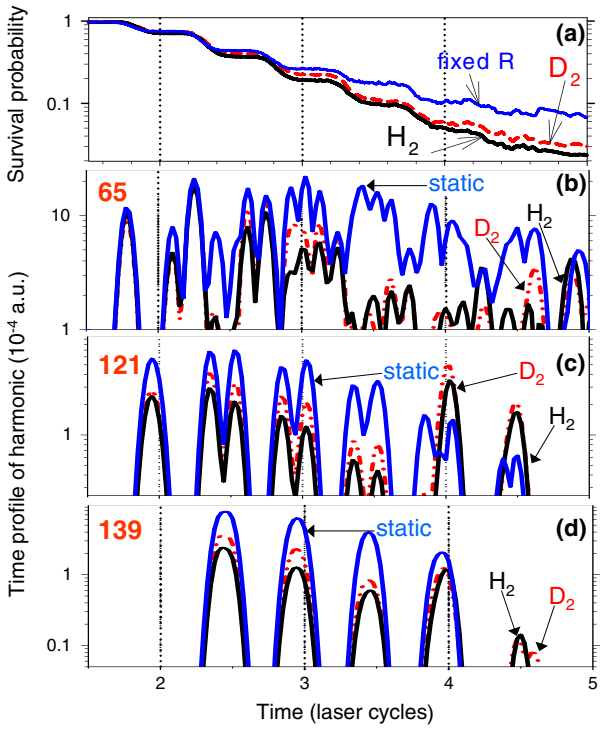

FIG. 2 (color online). (a) Survival probability defined as probability to find both electron close to nuclei at $|z_k| < 6$ a.u. (b)–(d) Time profile of harmonics (65th, 121th, and 139th) $|d_G(\omega, \beta)|$ obtained using the Gabor transform [11] for D_2 molecule (red-dashed), H_2 molecule (solid black), and for the static case (solid-blue), i.e., for R fixed at $R = R_e = 1.7$ a.u..

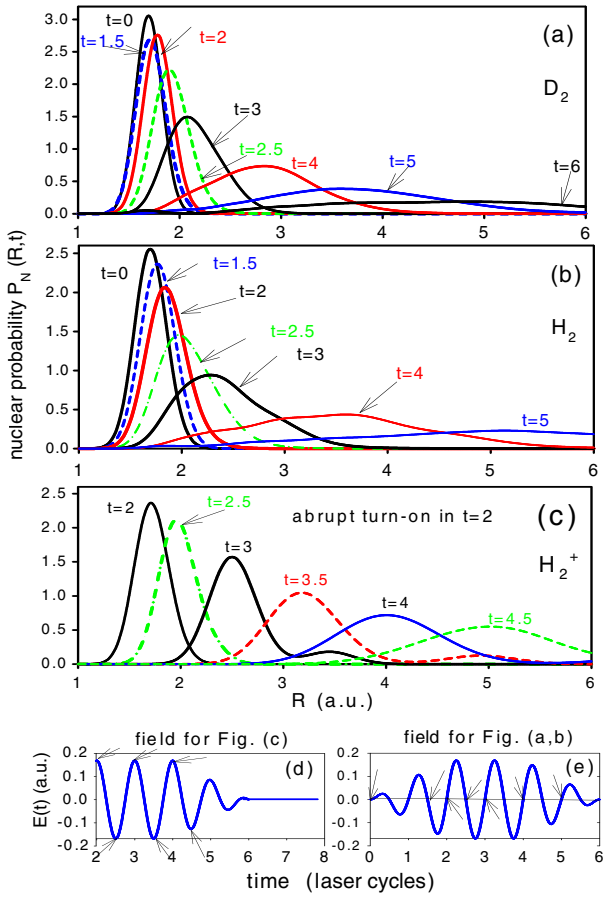

FIG. 3 (color online). Nuclear probabilities $P_N(R, t)$ obtained from TDSE for (a) D_2 molecule, (b) H_2 molecule, and (c) for a H_2^+ molecule using the FC initialization [14]. In the case (c) we solve the TDSE for a 1D, H_2^+ molecule, as in [14].

for which enhanced ionization, CREI, helps to see the contribution of the second electron. At $t = 4$ cycles the nuclei have already moved to $R > 3$ a.u. where the ionization rates in H_2^+ reach maximum; see Figs. 3 and 4. From the experimental point of view, in general, it is difficult to see harmonics from second ionization due to plasma effects. However, the experiments in hollow fibers allow to see the contribution from such second ionization electrons [15], i.e., from H_2^+ in the present case.

Further insight into the nuclear motion signature is illustrated in Fig. 3 which shows the nuclear wave packets probabilities $P_N(R, t)$. Figures 3(a)–3(c) shows the probability $P_N(R, t)$ as a function of R calculated at consecutive time intervals equal to half-cycles of the laser pulse. Because of the very high laser intensity, $I = 10^{15}$ W/cm^2, the nuclear motion is very fast even in the case of the heavier D_2 isotope, Fig. 3(a), which advances up to $R = 3$–3.5 a.u. during the first 4 cycles (1-laser cycle = 2.67 fs) right at the time when the laser pulse starts its turn-off, see Fig. 3(e), and H_2 advances clearly further (over 0.5 a.u.). The nuclear wave packet broadens considerably at this time due to the spread in ionization times of the first electron occurring at several consecutive first half cycles. One may expect that at this very high laser intensity the most likely time for creation of the H_2^+ molecule is at $t = 2$ laser cycles when the laser pulse reaches a maximum and that for later times the dissociating H_2^+ contributes significantly to the harmonic generation. In order to confirm this we plot in Fig. 3(b) the solutions of the one electron TDSE for H_2^+ initialized at $t = 2$ cycle. The H_2^+ initial nuclear wave function on the ground Σ_g surface is assumed to be the $v = 0$ vibrational state of H_2, in other words words, an instantaneous Franck-Condon (FC) transition is assumed to occur at $t = 2$ cycles, followed by exact non-Born-Oppenheimer (one electron + two protons) dynamics. Clearly, peaks of nuclear proba-

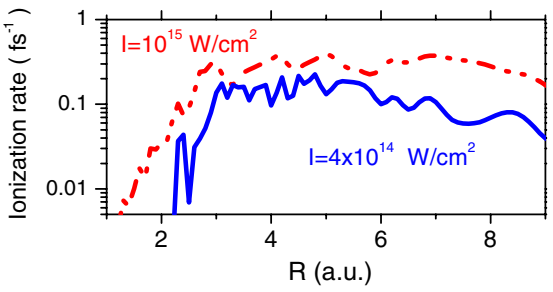

FIG. 4 (color online). Static ionization rates of a H_2^+ molecule as function of internuclear distance R.

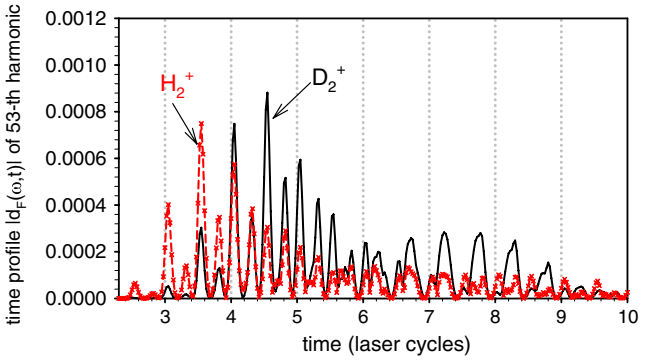

FIG. 5 (color online). Time profiles $|d_G(\omega = 53\omega_L, t)|$ obtained from TDSE for H_2^+ and D_2^+, using the FC initialization [14] [as in Fig. 3(c)], for a pulse similar to that in Fig. 3(e) but with a 16-cycle constant envelope, and $I = 4 \times 10^{14}$ W/cm^2.

bilities shown in Fig. 3(c) move with similar speed as peaks obtained from the exact 2-electron, 2-proton dynamics shown in Fig. 3(b). This means that the second electron will contribute to the MHOHG process at $t > 3$ cycles when the first electron ionization has been completed. The most remarkable result (for the 65th harmonic shown in Fig. 2(b)] is that the MHOHG process in H_2 essentially stops after 3 laser cycles and is produced mainly at 2.25 and 2.75 cycles in spite of a 6-cycle duration of the pulse. Note, that for a D_2 molecule MHOHG stops a half- cycle later than in H_2, whereas in the static case (with R frozen at $R_e = 1.7$ a.u.) the harmonics are generated until the moment when the pulse starts its turn-of at $t = 4$ cycle. This clear shortening of the train of attosecond pulses in H_2 molecule for times >3 cycles can be traced to the following main mechanism: significant enhancement of ionization rates at $R > R_e$ a.u. in a neutral molecule leading to the faster depopulation of the initial state than in a static molecule. The ionization rate at $R \simeq 3$ a.u. in H_2^+ is over 1 order of magnitude higher than the rate at $R \simeq 2$ a.u. for intensities $I > 4 \times 10^{14}$ W/cm^2 at $\lambda = 800$ nm. Thus any H_2^+ created by the first ionization of H_2 will undergo further ionization and concomitant Coulomb explosion [14]. We see in Figure 3(b) that for $t > 3$ cycles the H_2 proton wave packet is already moving into this region and at $t = 4$ cycles its wave packet is completely dispersed, in part by Coulomb explosion. Nuclear motion also weakens MHOHG efficiency with respect the static system via an attenuating vibrational autocorrelation factor introduced in [10]. This factor is in part responsible for stronger harmonic peaks in D_2 than in H_2 seen in Fig. 1 but would rather not lead to the sharp shortening of the time profiles seen in Fig. 2.

So far our study has been restricted to the extremely intense and very short pulses. The interpretation of the obtained time profiles was complicated because of the contribution of two electrons. In order to confirm the above conclusions and interpretation regarding the shortening of the attosecond-pulse trains we present in Fig. 5 the time profile of a selected 53th harmonic, obtained from the TDSE for simpler, one electron systems, H_2^+ and D_2^+, initialized from the $v = 0$ vibrational state of H_2 (or D_2) placed on the H_2^+ Σ_g electronic surface. We use in Fig. 5 a longer pulse, similar in shape to that in Fig. 3(e) but with 16-cycle constant envelope and $I = 4 \times 10^{14}$ W/cm^2. Figure 5 clearly shows that the attosecond-pulse train is significantly shorter in H_2^+ than in D_2^+ and that the attosecond train contains just few strong individual attosecond pulses. Moreover, the strongest individual attosecond-pulse occurs in H_2^+ one cycle earlier than in D_2^+. This means that by measuring the temporal shape of the pulse train we are able to monitor the nuclear motion.

In summary, our non-Born-Oppenheimer TDSE simulations of MHOHG in the H_2, H_2^+ systems show that two important factors related to the nuclear motion regulate molecular high-order harmonic generation: (i) rapid enhancement of the ionization rate of both the neutral and of the ion as a function of R; (ii) rapid movement and broadening of both ion and neutral molecule nuclear wave packets during the pulse. These two effects operate in concert leading to the generation of shorter trains of attosecond pulse in fast dissociating light molecules than in molecules with frozen nuclear motion (or than in atoms). High intensity pulses ($I \simeq 10^{15}$ W/cm^2) will therefore produce harmonics efficiently only at the beginning of the pulse as a result of enhanced ionization and concomitant nuclear motion.

We thank Myriam Ziou for help with figure preparation.

[1] P. B. Corkum and F. Krausz, Nature Phys. **3**, 381 (2007).
[2] A. D. Bandrauk *et al.*, in *Prog. in Ultrafast Intense Laser Science*, edited by K. Yamanouchi *et al.* (Springer, NY, 2007), Vol. III, Chap. 9.
[3] P. Agostini and L. F. DiMauro, Rep. Prog. Phys. **67**, 813 (2004).
[4] P. B. Corkum, Phys. Rev. Lett. **71**, 1994 (1993).
[5] T. Zuo and A. D. Bandrauk, Phys. Rev. A **52**, R2511 (1995).
[6] T. Seideman, M. Y. Ivanov, and P. B. Corkum, Phys. Rev. Lett. **75**, 2819 (1995).
[7] P. H. Bucksbaum *et al.*, Phys. Rev. Lett. **64**, 1883 (1990).
[8] J. Itatani *et al.*, Nature (London) **432**, 867 (2004).
[9] S. Baker *et al.*, Science **312**, 424 (2006).
[10] M. Lein, Phys. Rev. Lett. **94**, 053004 (2005).
[11] P. Antoine, B. Piraux, and A. Maquet, Phys. Rev. A **51**, R1750 (1995).
[12] T. Kreibich *et al.*, Phys. Rev. Lett. **87**, 103901 (2001).
[13] A. D. Bandrauk and H. Z. Lu, Phys. Rev. A **72**, 023408 (2005).
[14] S. Chelkowski, C. Foisy, and A. D. Bandrauk, Phys. Rev. A **57**, 1176 (1998).
[15] E. A. Gibson *et al.*, Phys. Rev. Lett. **92**, 033001 (2004).